Journal of Food Engineering 404 (2026) 112773

Contents lists available at ScienceDirect

Journal of Food Engineering

journal homepage: www.elsevier.com/locate/jfoodeng

Thermodynamic model and infrared thermography monitoring system for convective drying of goldenberry (*Physalis peruviana*)

T. Chuquizuta [a,b], W. Castro [c], M. Castro-Giraldez [a], P.J. Fito [a,*]

[a] Instituto Universitario de Ingeniería de Alimentos FoodUPV, Universitat Politècnica de València, Camino de Vera s/n, Valencia, 46022, Spain
[b] Instituto de Investigación del Mejoramiento Productivo, Universidad Nacional Autónoma de Chota, Chota, 06120, Peru
[c] Facultad de Ingeniería de Industrias Alimentarias y Biotecnología, Universidad Nacional de Frontera, Sullana, 20100, Peru

ARTICLE INFO

Keywords:
Thermodynamic
Infrared thermography
Physalis
Drying and monitoring

ABSTRACT

The goldenberry (*Physalis peruviana*) is a highly perishable Andean fruit with valuable nutritional and functional properties. Its preservation poses a challenge due to its high moisture content. This study presents an integrated method combining infrared thermography (IR) and irreversible thermodynamics to characterize the convective drying process of goldenberry.Samples were dried at 60 °C and 1.0 m/s air velocity. Weight loss, surface temperature, and water activity were recorded over 13 h using thermocouples, precision balances, and IR imaging. An irreversible thermodynamic model was applied to estimate water flux, free energy changes, and chemical potential gradients, including mechanical energy effects. The phenomenological coefficient from Onsager's relation was correlated with water flux to describe internal water migration. IR thermography enabled real-time, non-invasive monitoring of temperature and emissivity, correlating with morphological changes during drying. Sorption isotherms were fitted using the GAB model, and thermodynamic analysis allowed separation of physical and mechanical contributions to water potential. This approach provides a deeper understanding of moisture transport during drying and demonstrates the usefulness of combining IR monitoring with thermodynamic modeling. It offers a promising tool for optimizing drying protocols in high-moisture tropical fruits like goldenberry.

1. Introduction

The goldenberry (*Physalis peruviana*), also known as uchuva (caspe goldberry or goldberry) in several Latin American countries, is a fruit that originated in the Andean region and is widely regarded as an exotic fruit, especially appreciated when consumed fresh (Bazalar Pereda et al., 2019; Blas Saavedra et al., 2024; Hidayat et al., 2021; Yıldız et al., 2015). The goldenberry is composed of 75–85 % (w/w) moisture, 11–16 g of carbohydrates, 0.3–1.9 g of protein, 0–0.5 g of fat, and 43 mg of ascorbic acid per 100 g of the edible portion (Puente et al., 2011; Rossi et al., 2012). The fruit contains various bioactive components, including vitamin C, β-carotenes, total phenols, phenolic acids, and flavonoids. These compounds confer beneficial properties to the consumer, such as anti-inflammatory effects. The goldenberry fruit has been demonstrated to possess antioxidant, anticarcinogenic, antidiabetic, and cardiovascular disease prevention properties (Ordóñez-Santos et al., 2017; Pasten et al., 2024; Vega-Gálvez et al., 2015). However, the physicochemical and nutritional properties of the fruit vary according to its stage of maturity and the technical and post-harvest conditions under which it is cultivated (Avendaño et al., 2022; Hidayat et al., 2021; Lopez et al., 2024; Muñoz et al., 2021).

In recent years, Colombia and Peru have emerged as prominent players in the marketing and export of fresh goldenberry fruits to Europe, Asia, and North America, driven by the fruit's recognised nutritional benefits for human health (Obregón La Rosa et al., 2021; Ramirez-Hernandez et al., 2020). However, due to the respiration rate (influenced by temperature), high moisture content and water activity, goldenberry fruits are considered highly perishable fruits and therefore have a limited shelf-life (Garavito et al., 2021). Additionally, they are susceptible to fungal and yeast contamination (Fischer et al., 2011; Fischer and Martinez, 1999), underscoring the necessity for preservation techniques aimed at reducing moisture content and, consequently, prolonging the shelf-life of the product (İzli et al., 2014).

Drying is a preservation method that is employed extensively in the agri-food sector, particularly in the context of fruit dehydration. This process enables the extension of fruit shelf-life by reducing moisture

* Corresponding author.
E-mail address: pedfisu@tal.upv.es (P.J. Fito).

https://doi.org/10.1016/j.jfoodeng.2025.112773
Received 16 May 2025; Received in revised form 21 July 2025; Accepted 6 August 2025
Available online 8 August 2025

content and water activity, thereby minimizing and/or inhibiting spoilage, enzymatic activity and microbial growth (Doymaz, 2008; Vásquez-Parra et al., 2013; Vega-Gálvez et al., 2015). Moreover, the process of fruit dehydration involves a series of concurrent operations, including mass and heat transfer (Lopez et al., 2013; Pasten et al., 2024), improving water diffusion conditions from the interior to the surface in contact with the circulating air has been demonstrated (Barbosa-Cánovas and Vega-Mercado, 1996; İzli et al., 2014; Vega-Gálvez et al., 2015). Consequently, this leads to changes and deterioration in the cell wall, collapse and stiffness (texture) of cell tissues (Cabrera Ordoñez et al., 2017; Nawirska-Olszańska et al., 2017; Vega-Gálvez et al., 2015).

Conversely, the convective drying method is more extensively employed in the agri-food industry, where numerous endeavours have been made to model the drying kinetics and ascertain the effective water diffusion of goldenberry fruits. The mathematical models most commonly used to predict the behaviour of drying kinetics are: Newton, Wang and Sing, Henderson-Pabis, Page, Logarithmic, Midilli and Kucuk (İzli et al., 2014; Junqueira et al., 2017; L. Puente et al., 2020, 2021; Uribe et al., 2022; Vega-Gálvez et al., 2014). In a similar vein, Yasin et al. (2016), Vásquez-Parra et al. (2013) and Vega-Gálvez et al. (2014) have obtained the effective diffusion assuming a finite plate and sphere geometry. However, it should be noted that the equations employed in modelling kinetics and determining effective diffusion have certain limitations, such as the failure to consider additional factors (such as relative humidity), variations in operating temperature and interactions between fruit components. Furthermore, the aforementioned equations are based on empirical and simplified models, which may have a detrimental effect on the accuracy of the calculations for the design of a dryer and the dehydration process.

Thermodynamics is the scientific study of energy transfer and mass movement during the process of food dehydration. In this context, the analysis of sorption isotherms is considered a fundamental tool for the design, modelling and optimization of technological processes (Aviara N, 2020; Kraiem et al., 2023). These isotherms are also pivotal in analysing the thermodynamic interactions between food components and water, as well as in quantifying the energy requirements of the dehydration process. Conversely, several researchers advocate the utilisation of the Guggenheim-Anderson-de Boer (GAB) and Brunauer-Emmett-Teller (BET) models to predict avocado sorption isotherms (Pasten et al., 2024; L. Puente et al., 2020; Vega-Gálvez et al., 2015; Vega-Gálvez et al., 2014). However, such predictions are often limited to parameters such as critical humidity, isosteric heat, entropy and enthalpy (Aviara N, 2020; Akpinar et al., 2006; Junqueira et al., 2017; Pasten et al., 2024; L. Puente et al., 2020; Ruan et al., 2022; Yasin et al., 2016). It is therefore necessary to study new thermodynamic variables such as exergy and the optimization of energy loss minimization, in order to enrich the understanding of the dehydration process.

Moreover, the examination of energy interactions and thermodynamic behaviour between air and food during dehydration in a drying chamber, based on the second law of thermodynamics, remains underexplored in the scientific literature. This paucity of research is due to the intricacy of studying enthalpy and exergy changes that occur in both reversible and irreversible processes (Akpinar et al., 2006; Talens et al., 2016a). The surface temperature of the food is a primary factor influencing these changes, arising from convective heat transfer. The most common method to measure the temperature of a food during dehydration is through the use of calibrated thermocouples (types K, T or Pt), data loggers and computers. However, this method is destructive and restricts temperature recording to a single point (Motahayyer et al., 2019; Yilmaz et al., 2008). Consequently, there is a clear need to develop non-destructive systems that facilitate the monitoring of surface temperature during fruit drying, thus improving upon the aforementioned problems (Kylili et al., 2014).

Recent studies have demonstrated the efficacy of infrared thermography (IR) as a valuable tool for two-dimensional, non-contact temperature diagnosis of biological materials during the drying process, providing relevant information on heat transfer (Kylili et al., 2014; Motahayyer et al., 2019; Traffano-Schiffo et al., 2014). The underlying principle of infrared thermography is the measurement of infrared radiation emitted by a surface, thereby generating an image of the thermal distribution (Gowen et al., 2010). This technology has been extensively employed in the control of processes such as the drying of pork (Traffano-Schiffo et al., 2014), potatoes (Tomas-Egea et al., 2021), coffee beans (Reyes-Chaparro et al., 2024), mushrooms (Lombraña et al., 2010), rice (ElGamal et al., 2017) and wood (Lerman and Scheepers, 2023). Its application in freezing potatoes (Cuibus et al., 2014) and water stress analysis in citrus (Pappalardo et al., 2023) has also been documented. However, there is a paucity of studies on its use in the drying of berries, such as grapes (Reyes-Chaparro et al., 2024), and even more so in tropical berries such as goldenberry.

The initial objective of this study was to provide a comprehensive overview of the advantages of the first and second laws of thermodynamics in the drying process, and to explore non-invasive methods of monitoring, such as infrared thermography. The subsequent aim was to develop a thermodynamic model to facilitate a more in-depth understanding of the mechanisms of internal heating and water transport in goldenberry fruit during hot air drying. This was to be achieved by monitoring the process with infrared thermography.

2. Materials and methods

The experimental procedure is shown in Fig. 1. Likewise, each step of the flowchart is explained in the following paragraphs. Each experimental condition was tested with three replicates (n = 3).

2.1. Sample goldenberry fruits

The samples of fresh goldenberry fruit at commercial ripeness, coming from Ecuador, were obtained through the importing company Ammarket (Orihuela, Alicante - Spain). The goldenberry fruits arrived in refrigerated boxes (100 g/box) with uniform size (diameter) and weight, 3.8 ± 0.21 cm and 3.9 ± 0.4 g, respectively, which were kept in a refrigerator at 6 °C until later analysis and execution of the experiment.

2.2. Sample conditioning

Before drying the goldenberry fruit, the skin of two fruits (for each replicate) was removed manually using tweezers. The fruit's moisture content (dry basis) was also characterized using the methodology of AOAC Method 934.06, 2000.

2.3. Drying process

Before drying, the works of (Cuibus et al., 2014; Talens et al., 2017; Traffano-Schiffo et al., 2014) were used as a reference to install and locate the following equipment in the dryer: a precision balance (Mettler Toledo PG503-S, Spain), a thermal imaging camera (infrared camera) (Optris PI® 160, Germany), a data logger (Agilent 34972A, Malaysia) and a desktop computer. In addition, type K thermocouples, reference emissivity material (ε = 0.95 - Optris GmbH, Germany), and graph paper (9 cm^2) were placed as shown in Fig. 2.

Two units of goldenberry fruit were placed in a convective dryer, and one of the fruits was suspended from a precision balance by means of a nylon thread to monitor the mass during 13 h of drying. The mass of the sample was recorded every 5 min during the first hour, every 10 min between the first and second hours, and every 15 min for the rest of the drying period. The second goldenberry fruit was also placed to the right of the suspended fruit, in order to measure the surface emissivity.

The convective dryer was operated at a temperature of 60 °C and a drying air velocity of 1.0 m/s (monitored with a Proster anemometer, model HT 383, China). During the drying process, the temperatures of

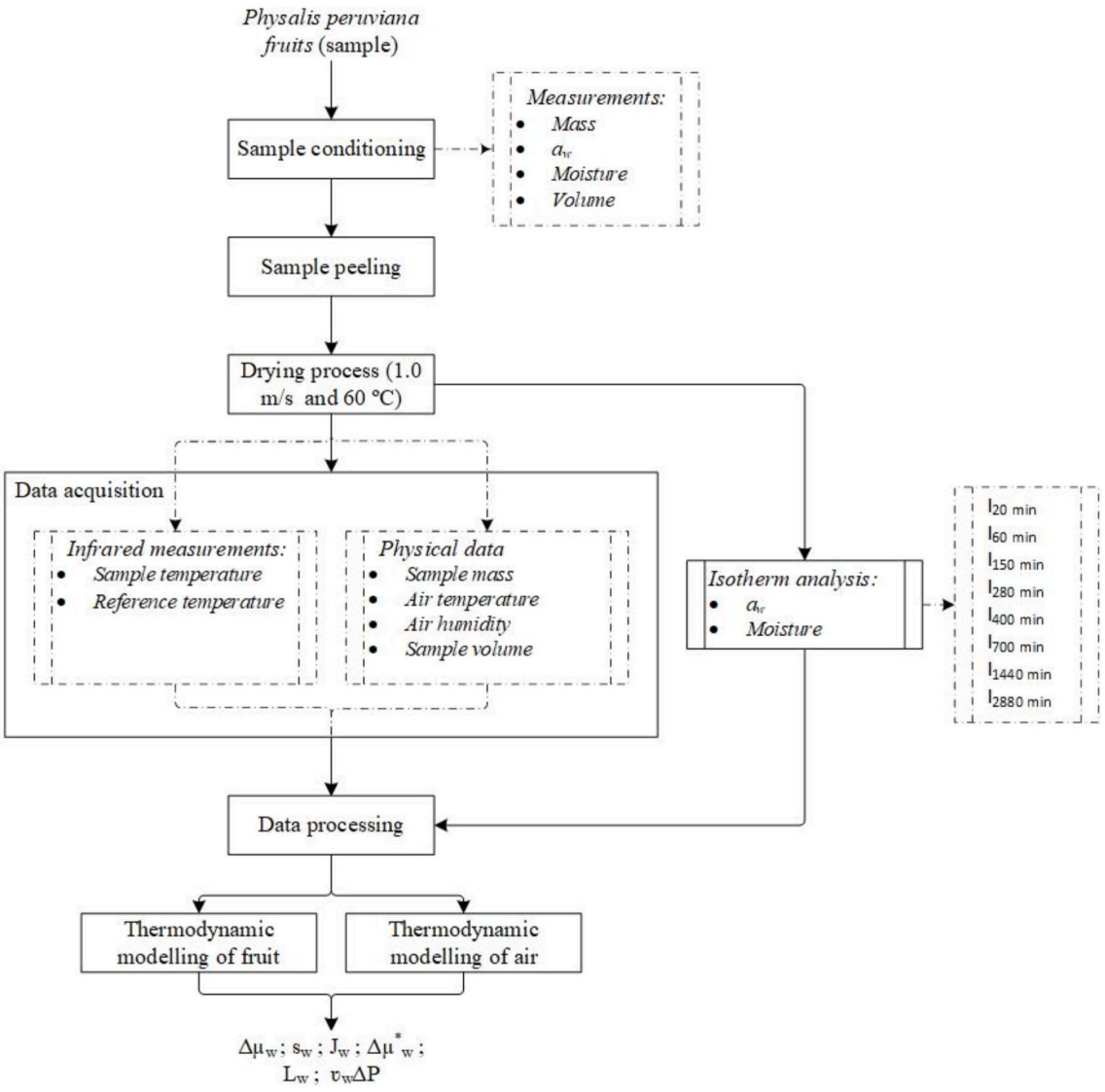

Fig. 1. Experimental procedure in drying process of *Physalis peruviana*.

the sample, drying air and reference emissivity material were recorded with thermocouples (connected to an Agilent 34901A multiplexer, Malaysia) to correct the emissivities recorded by the thermal camera. Dehydration was performed in triplicate.

2.4. Infrared thermography

According to (Tomas-Egea et al., 2022; Traffano-Schiffo et al., 2014), in order to obtain thermal images, the thermal camera operates under the following conditions: two-dimensional focal plane (matrix) of 160 × 120 pixels, spectral range of 7.5–13.0 μm, resolution of 0.05 °C and accuracy of ±2 %. The thermal camera measures in a temperature range of −20 to 900 °C, with a field of view (FOV) of 23° × 17° at a minimum distance of 20 mm and a frame rate of 120 Hz, which is connected to a desktop computer to record thermal images throughout the drying process using the Optris PI Connect software (Optris GmbH, Berlin, Germany). Similarly, the reference emissivity material (radius = 12.5 mm and ε = 0.95) was placed parallel to the lens of the thermographic camera at a distance of 40 cm to calculate the reflected energy received by the thermographic camera.

2.5. Sorption isotherm modelling

In parallel with the drying process and under the same operating conditions, a convection dryer was used to dehydrate 24 fresh skinless goldenberry. The masses of the samples were previously determined using a precision balance (Mettler Toledo AB304-S), then each sample was placed on each Petri dish and arranged in three rows and eight columns. Each column corresponds to a different drying time and isothermal curve (see Fig. 1), from which the samples were taken out of the dryer and allowed to stabilize for 30 min to record their mass and water activity (Aqualab®, Series 3 TE). The samples were then kept at 4 °C for 24 h, and after the equilibration process, the mass, water activity, and moisture of the equilibrated samples were measured (Traffano-Schiffo et al., 2015).

The experimental moisture values and their respective water activities were adjusted with the GAB model by Equation 1

$$X_W = \frac{X_{W0}\, C\, a_w}{(1 - K\, a_w)(1 + (C-1)a_w)} \quad (1)$$

Where: X_w corresponds to the sample moisture (kg_w/kg_{dm}), X_{w0} the monomolecular moisture layer (kg_w/kg_{dm}), C corresponds to the Guggenheim constant (dimensionless) and K is the correlation factor

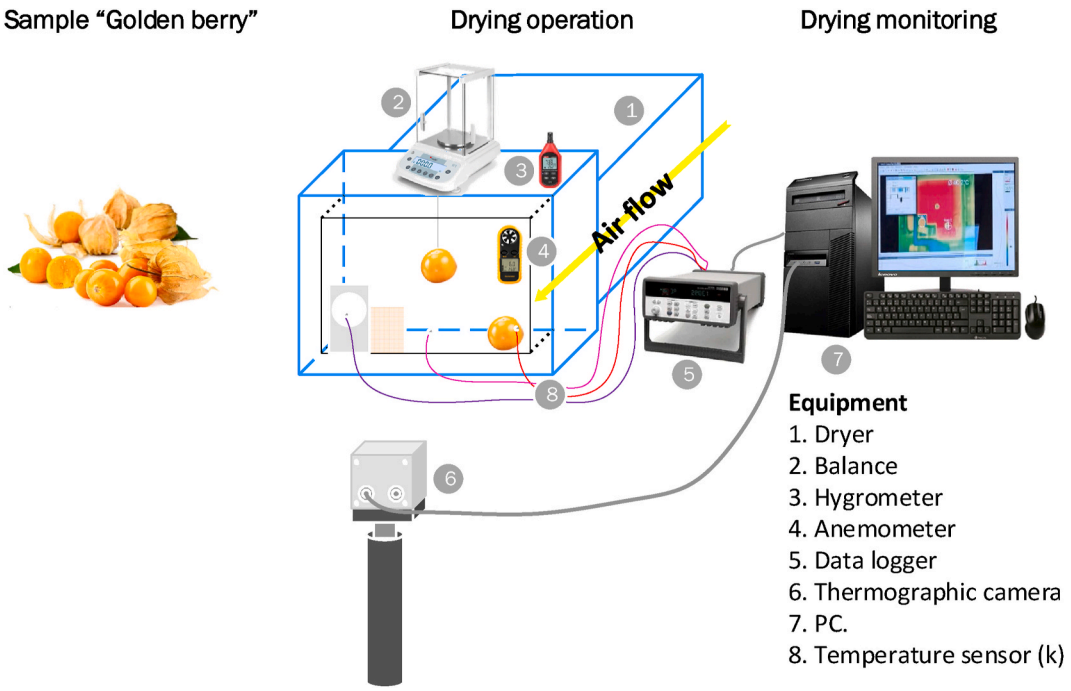

Fig. 2. Equipment for convective drying operation of Physalis peruviana must be assembled.

(dimensionless).

2.6. Differential scanning calorimetry (DSC)

The methodology proposed by (Vega-Gálvez et al., 2014a), with slight modifications, was used to determine the heat capacity (Cp) of fresh goldenberry samples. The thermal profiles of the samples were obtained using a differential scanning calorimeter (DSC, System 1 StareE, Mettler-Toledo, Switzerland), which was calibrated using the automatic calibration function FlexCal, as recommended by the manufacturer. Each sample (10–15 mg) was weighed directly into a 40 μL DSC aluminium pan (Mettler Toledo, ME-00026763) using a Mettler Toledo XS-205 balance, excluding the mass of the pan. The pan was then hermetically sealed to prevent moisture loss during the analysis. The sample pans, along with an empty pan used as a reference, were placed in the DSC oven. All experiments were performed in triplicate, following the thermal profile described below: samples were cooled from room temperature to −50 °C at a rate of −5 °C/min and held at this temperature for 30 min to ensure complete freezing. Subsequently, the samples were heated from −50 °C to 80 °C at a rate of 10 °C/min, and held at 80 °C for 1 min.

3. Results and discussion

3.1. Drying kinetics of Physalis peruviana

To better understand the drying kinetics of goldenberry, it is essential to first describe the internal tissue structure through which water is transported. The fruit consists of approximately 1 % epidermal tissue (which is removed prior to drying), around 15 % cortical parenchyma near the skin, 3 %–5 % vascular tissue, and between 70 % and 85 % spongy parenchyma, with the remainder corresponding to seeds (Balaguer et al., 2024). These anatomical features imply that water transport involves multiple coordinated pathways: apoplastic (extracellular), symplastic (intracellular, via plasmodesmata), and transmembrane (connection extra and intra cellular transport), all primarily occurring within parenchymal tissues. The coexistence of these transport mechanisms, along with structural events such as plasmolysis, results in multiple internal water transport rates operating simultaneously during drying.

Fig. 3 shows the classic drying curve of the goldenberry sample, which started with an initial moisture of 4.102 ± 0.043 (kg_w/kg_t) and reached a final moisture of 0.298 ± 0.108 d.b. in 13 h of continuous drying, corresponding to a mass loss of 74.55 % (±2.11). It should be noted that the surface moisture of the goldenberry sample evaporates first, then the water moves from the inside of the sample to the surface by diffusion principles (Doymaz, 2008), in agreement with the work reported by (Vásquez-Parra et al., 2013; Lopez et al., 2013).

Nevertheless, given the inherent difficulty in observing the drying stages undergone by the goldenberry, it is essential to plot the drying speed curve (Fig. 4) in order to gain insight into this process.

The drying rate curve illustrates the variation in drying rate in relation to the dry-base moisture content and allows the observation of three distinct drying phases. A brief induction phase (I) is evident during the initial three points, succeeded by a phase of constant drying rate (II)

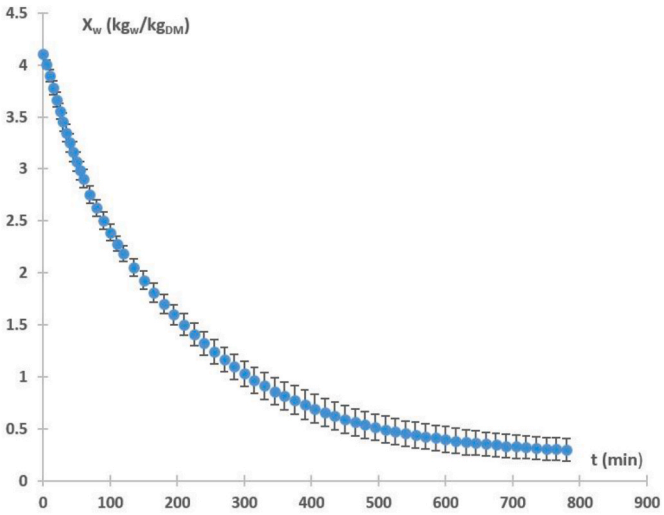

Fig. 3. Drying curve of *Physalis peruviana* at 60 °C.

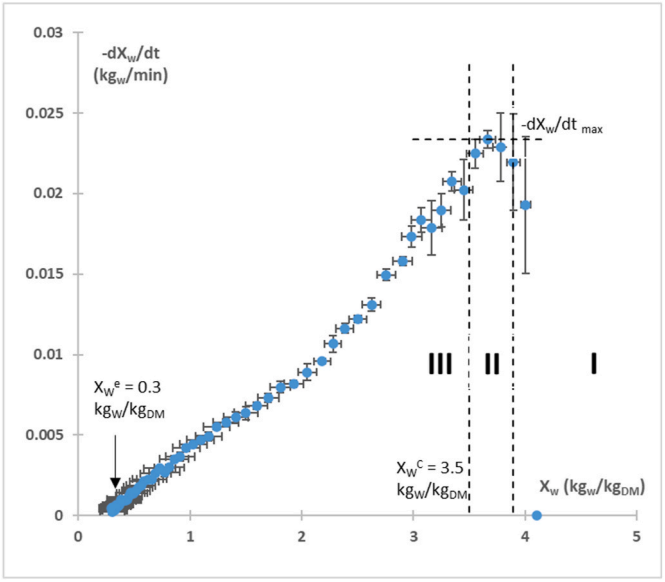

Fig. 4. Drying speed of *Physalis peruviana*; drying stage: I - induction, II – constant drying rate and III – decreasing drying rate.

at 0.024 kg_w/min with a critical moisture content of 3.5 kg_w/kg_{DM}. Subsequent to the critical moisture content, a decline in the drying rate is observed until equilibrium moisture is reached (0.3 kg_w/kg_{DM}), which occurs 45 min after the commencement of the drying process.

Additionally, during the drying process, the goldenberry exhibits deformation associated with water loss and morphological transformations resulting from internal cellular plasmolysis of the fruit, as evidenced by volume variation (Fig. 5).

Goldenberry consists mainly of parenchymatic tissue, characterized by thin primary cell walls, high vacuole content, and loosely packed cells. During drying, the removal of water from this tissue leads to plasmolysis, collapse of cell walls, and progressive loss of turgor pressure. These structural changes contribute to the distinct phases observed in the drying rate curve. In the initial constant-rate period, free water from intercellular spaces and vacuoles is easily evaporated. As drying progresses and water must diffuse through increasingly rigid and collapsed cell matrices, the drying rate decreases, marking the transition to the falling-rate period.

It is important to note that the loss of volume is directly proportional to the water loss, resulting in an overall volume reduction of 68 %. If the tissue volume were to shrink exactly in proportion to the volume of water lost, the expected shrinkage would be approximately 95 %. However, part of the space formerly occupied by water becomes filled with air, leading to a partial swelling or expansion of the tissue matrix.

The drying process is a complex operation, and existing empirical and/or physical models are inadequate for describing and explaining the transfer of mass and heat in the dehydration of food. In recent studies such as Traffano-Schiffo et al. (2014), Talens et al. (2016a, 2016b) and Frutaz et al. (2025), the importance of using irreversible thermodynamics to describe the phenomenon of water transport during drying based on the structure of the food has been demonstrated. Therefore, it is crucial to determine the flow of water extracted from the fruit using Equation (2).

$$J_W = \frac{\Delta M_w \cdot M_0}{\Delta t \cdot S\, Mr_W} \tag{2}$$

In this equation, ΔM_w represents the mass variation of water in the sample, M_0 denotes the initial mass, Δt signifies the variation in drying time, and S is the surface obtained from the volume (Fig. 5), assuming that the goldenberry is a sphere. M_{rW} represents the molecular mass of water (18 g/mol).

Fig. 6 shows the water flow extracted from the goldenberry sample exhibits an increase until reaching 0.01831 ± 0.00089 ($kmol_W/m^2$ s), which is caused by the appearance of the drying induction stage and is almost non-existent in other fruits. Once the drying induction stage is complete, the water flow declines throughout the remainder of the drying process, reaching a final value of 0.000611 ± 0.000091 ($kmol_W/m^2$ s), as anticipated, coinciding with work carried out on samples of goldenberry by (Vega-Gálvez et al., 2014b; Vega-Gálvez et al., 2014).

3.2. *Thermographic monitoring of the drying process of Physalis peruviana*

The importance of monitoring the temperature variation in the boundary layer between the surface temperature of the goldenberry sample and the temperature of the drying air using a thermal imager during the drying process allows the surface phenomena affecting drying to be identified and described (Traffano-Schiffo et al., 2015). It should be noted that the thermal imager detects the energy flow through its pyroelectric detector, which is based on the Stefan-Boltzmann law for heat transfer by radiation (Talens et al., 2017).

In order to interpret the measurements of the radiant energy flux recorded by the thermal camera, and therefore calculate the emissivity

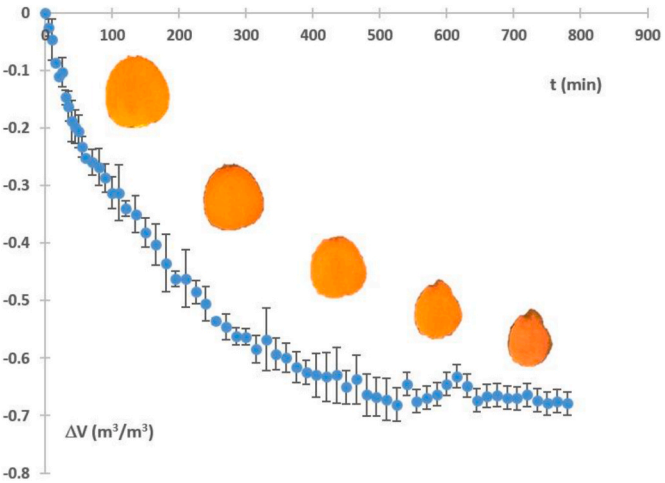

Fig. 5. Volume variation curve of *Physalis peruviana* during the drying process at 60 °C.

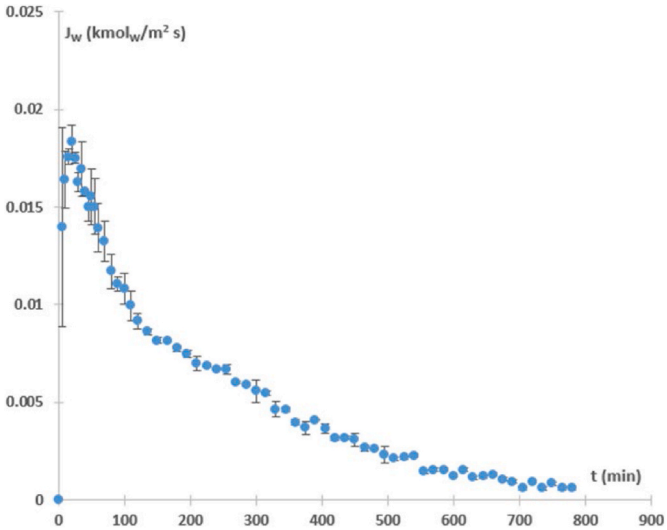

Fig. 6. The evolution of water flux during the drying process of *Physalis peruviana*.

of the goldenberry sample during drying, it is important to carry out a radiant energy balance based on the Stefan-Boltzmann law, taking into account the following terms: the first term represents the energy flux emitted by the goldenberry sample, the second term represents the energy flux emitted by the environment and the third term represents the energy flux absorbed by the air (Traffano-Schiffo et al., 2014), see Equation (3).

$$E_T = \varepsilon_C \sigma {T_C}^4 = F \cdot \varepsilon_{obj} \sigma T_{obj}^4 + E_{env} - (1 - \tau_{air}) F \cdot \sigma T_{air}^4 \quad (3)$$

Where E_T is the total energy received by the camera (W/m^2), ε_C is the emissivity set in the thermographic camera ($\varepsilon_C = 1$), σ is the Stefan-Boltzman constant (5.67 × 10^{-8} W/m^{2}K^4), T_C is the temperature calculated by the thermographic camera, F is the geometric factor that can be taken as 1 when the camera is placed perpendicular to the samples, ε_{obj} is the emissivity of the goldenberry, T_{obj} is the surface temperature of the golden berry, E_{env} is the energy of the environment on the object obtained with the reference material, τ_{air} is the air permeability which, when it is less than 40 cm from the fruit and the RH of the environment is less than saturation, can be considered equal to 1, leaving this term as zero.

As observed in Fig. 7, the average emissivity of the goldenberry sample decreases to a value of 0.834 ± 0.070 during the first 45 min, this phenomenon is due to the absorption of radiant energy by the water molecules present on the surface of the goldenberry sample (degree of excitation) in the infrared range, therefore as the humidity decreases, its emissivity will be lower, in agreement with that reported by (Traffano-Schiffo et al., 2014) in the dehydration of pork. After the critical drying humidity (45 min), which is the beginning of the decreasing drying stage, the drying rate decreases due to the decrease in the water flow from the center to the surface of the sample, as well as the mobility (diffusion) of the soluble solids (Uribe et al., 2022; Vega-Gálvez et al., 2014). It is also noteworthy to observe the effect of temperature on the emissivity, the latter increasing to 0.889 ± 0.015 as the temperature of the sample surface increases after 13 h of drying.

Once the surface temperature of the goldenberry sample was obtained, it was compared with the evolution of the air temperature during drying using a Mollier psychrometric chart. Fig. 8 shows two examples in different atmospheric conditions (cold and hot day) that cause the surface temperature of the goldenberry samples to change through different isenthalpic conditions, as observed in the orange peel drying process (Talens et al., 2016a, 2016b, 2017).

These two examples in Fig. 8, as limits of the experiment (cold and warm day), start the drying process with enthalpies of 16 and 20 kCal/kg$_{DA}$. It can also be seen that the drying process is initially adiabatic. The surface temperature of the sample starts from the wet temperature and rises to the drying temperature. However, the sample undergoes adiabatic heating and cooling as it approaches the drying temperature.

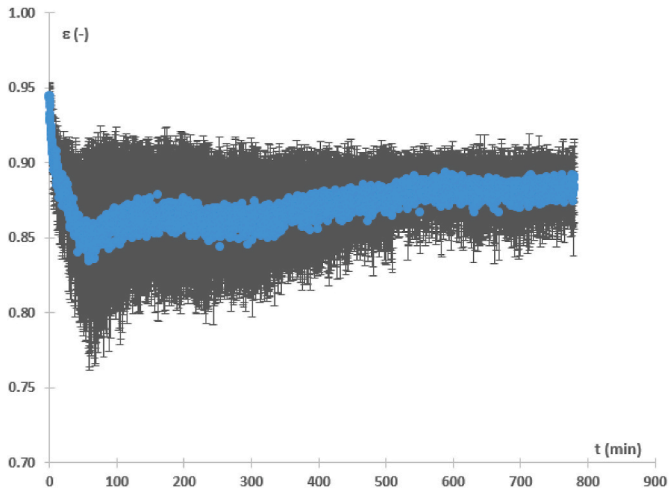

Fig. 7. Evolution of the mean emissivity values during the drying process of *Physalis peruviana*.

3.3. Sorption isotherm of Physalis peruviana

In order to determine the mechanisms that intervene and affect the drying (boundary layer), it is first necessary to obtain the relationship between humidity and water activity, so the sorption isotherm was carried out. The experimental data of the sorption isotherms of goldenberry at a temperature of 60 °C are shown in Fig. 9.

From the experimental data of the sorption isotherm, the values of: X_{w0}, C, K, Δ0, τ, α and ef have been obtained according to the GAB model, allowing a direct relationship between water activity and humidity based on the Gompertz transformation during drying, see Table 1.

The GAB model parameters provide insights into the water-binding behavior of goldenberry during drying. The monolayer moisture (X_{w0}) represents the amount of water adsorbed to specific active sites on the fruit surface, which is essential for product stability. A low X_{w0} indicates that goldenberry retains a relatively small amount of adsorbed water, consistent with its high sugar and acid content. The Guggenheim constant (C) reflects the strength of interaction between the first layer of water molecules and the food matrix. Higher C values suggest stronger binding forces. The K parameter accounts for multilayer water sorption beyond the monolayer; values of K closer to 1 indicate more homogeneous multilayer water binding. These parameters collectively help to understand the moisture adsorption and desorption behavior of goldenberry, relevant for optimizing storage and drying strategies.

In Table 1, GAB parameters have been compared with previous parameters obtained by Cortes et al. (2012). Compared to the data reported by Cortes et al. (2012), the monolayer moisture values obtained in this study appear more consistent with the expected behavior of fruits, which generally exhibit a lower water adsorption capacity than other foods such as meat. The values of parameter C are similarly low in both studies, indicating moderate isosteric heat values that align with the limited ability of fruit tissues to bind water molecules. In contrast, the K parameter typically approaches 0.99 in fruits, due to the steep slopes observed in isotherm curves under high turgor conditions, an aspect that appears inconsistent with the values reported by Cortes et al. (2012).

3.4. Thermodynamic modeling of drying of Physalis peruviana

The irreversible thermodynamics has the ability to describe the mechanical phenomena involved in the drying process of goldenberry; that is, it takes into account the structure of the food in the transport of water during drying and its interaction with the air (Fig. 10). In order to better understand the behaviors involved in the drying process, a thermodynamic model, based in the free energy variation, was developed and described by Equation (4) (Talens et al., 2016a).

$$dG = -SdT + VdP + Fdl + \psi de + \sum_i \mu_i \, dn_i \quad (4)$$

Where: SdT corresponds to the entropic term and is related to the heat flows; VdP corresponds to the mechanical energy term related to the pressure variation; Fdl corresponds to the mechanical energy term related to the tensile force; ψde corresponds to the energy term related to the electric field induced by the dissolved ions; $\sum_i \mu_i \, dn_i$ corresponds to the activity term and is the sum of the chemical potential of the species "i", the rest of the state variables being constant.

Considering the hypothetical existence of an interface between the air flow and the surface of the goldenberry, it is possible to calculate the increase in free energy between the two systems. Furthermore, in order to determine the driving force for water transport, it is necessary to obtain the water chemical potential, where it is defined as the free en-

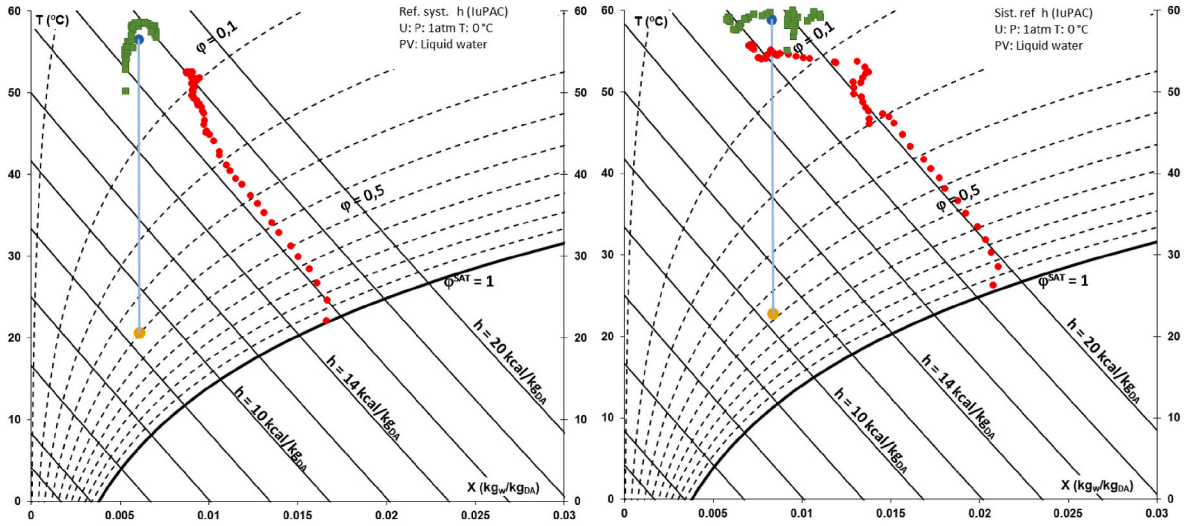

Fig. 8. Evolution of the mean emissivity values during the drying process of *Physalis peruviana*.

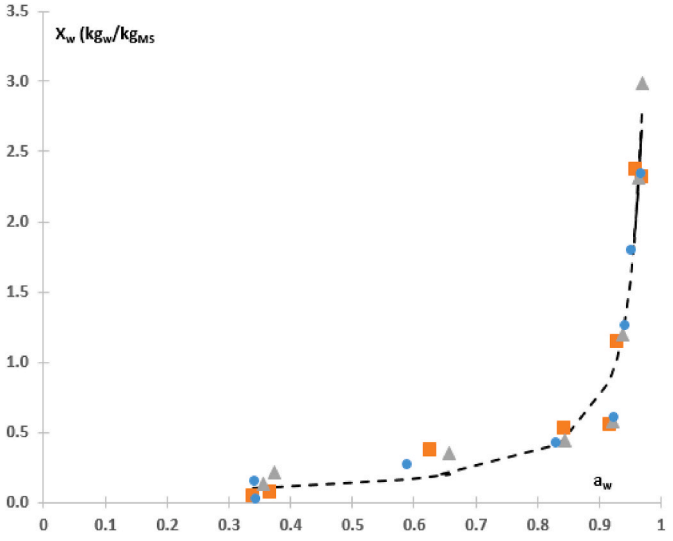

Fig. 9. Sorption isotherm of Physalis peruviana carried out in triplicate, where: ■ corresponds to the first experiment, ▲ corresponds to the second experiment and ●corresponds to the third experiment.

Table 1
GAB and Gompertz model parameters.

GAB (60 °C)				Gompertz (60 °C)	
$X_W = \frac{X_{W0}\, C\, a_w}{(1-K\,a_w)(1+(C-1)a_w)}$				$a_w = e_f + \frac{\Delta 0}{1+\left(e^{\tau^2 - \log(X_w)^2 \cdot \alpha}\right)}$	
Parameters	Experimental	(Cortés et al., 2012)	(Vega-Gálvez et al., 2014b)	Parameters	Experimental
X_{w0}	0.067	0.231	0.086	**Δ0**	0.8
				τ	−1.0
C	4.678	2.419	32.88	**α**	1.4
K	1.006	0.760	0.956	**ef**	1.1

ergy per mol of water (Equation (5)).

$$\Delta\mu_w = \frac{\Delta G}{\Delta n_w} \tag{5}$$

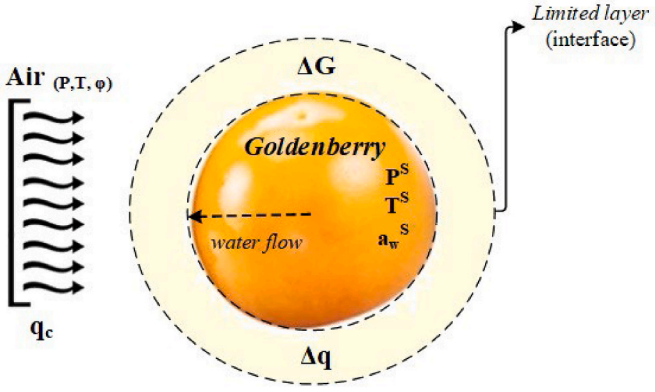

Fig. 10. Schematic diagram of the thermodynamic equilibrium.

Where: $\Delta\mu_w$ = water chemical potential (J mol^{-1}); ΔG = Gibbs free energy change (J); Δn_w = moles of water (mol). Equation (6) is obtained from equations (4) and (5). The terms *Fdl* and ψ*de* in equation (4) can be neglected, since the plant tissue is a rigid system and there is no great effect of ions, since the sample contains only native ions of goldenberry.

$$\Delta\mu_w = -s_w\left(T^{air} - T^S\right) + v_w\left(P^{air} - P^S\right) + RT^S \ln\frac{a_w^S}{\varphi^{air}} \tag{6}$$

Where: s_w = partial molar entropy of water (J K^{-1} mol^{-1}); T = temperature (K); υ_w = partial molar volume of water (m^3 mol-^{1}); P = pressure (atm); R = ideal gas constant (8.314472 J K^{-1} mol^{-1}); a_w = water activity; φ = relative humidity. The superscripts *s* and *air* refer to the surface of the goldenberry and the surrounding air, respectively.

Before obtaining the extended chemical potential of water, it is necessary to calculate the partial molar enthalpy of water (Equation (7))

$$s_w = \frac{C_p\cdot\left(T^S - T^{air}\right)\cdot M_t + \Delta G_{vap}\cdot M_0\Delta M_w}{M_t\cdot T^S\cdot x_w\cdot Mr_W} \tag{7}$$

Where: C_p = specific heat of goldenberry 3.96 ± 0.02 kJ kg^{-1} K^{-1} obtained by differential scanning calorimetry explained in material and methods section; T^s = surface temperature of the sample (K); T^{air} = temperature of the air surrounding the goldenberry (K); M_t = mass of goldenberry at each time of the drying process (kg); ΔG_{vap} = latent heat of vaporization 2494.4 kJ kg^{-1} (Fletcher, 1970); M_0^m = initial mass of the sample (kg); ΔM_w = mass variation of water in the sample during

drying (−); x_w = mass fraction of water in the sample during drying (kg kg-1); Mr_W = molecular mass of water (18 g mol^{-1}).

However, the limited information on the mechanical energy ($v_w\Delta P$) of the goldenberry fruit during the drying process makes it impossible to calculate all the terms of the chemical potential of water. It is therefore necessary to relate the available information to the water flow.

As the system is unstable and out of equilibrium, it is essential to understand the water flow and the thermodynamic forces involved in drying. The first Onsager relation (Traffano-Schiffo et al., 2014) can be used to describe the molar flow of water from the food, driven by the gradient of the chemical potential of water between the interior and the surface (Equation (8)). The phenomenological coefficient is constant in reversible processes and helps to quantify how easily water moves in response to this gradient. However, if mechanical energy stores cause irreversible fractures in the medium, the phenomenological coefficient will evolve according to the transformation undergone by the tissue.

$$J_w = L_W \cdot \Delta\mu_w \tag{8}$$

Where: J_w = molar flow of water (mol s^{-1} m^{-2}); L_w = phenomenological coefficient (mol^2 J^{-1} s^{-1} m^{-2}); $\Delta\mu_w$ = chemical potential of water (J mol^{-1}).

Since it is not possible to obtain the mechanical gradient, it is possible to calculate the rest of the components of the chemical potential of water. That is, a chemical potential can be defined without the effect of mechanical transformations in transport, using the following Equation (9) obtained from Equation (6).

$$\Delta\mu_w^* = -s_w\left(T^{air} - T^S\right) + RT^S \ln\frac{a_w}{\varphi^{air}} \tag{9}$$

Although it is not possible to obtain the mechanical gradient in the figure, it is possible to calculate the remaining components of the chemical potential of water. That is, a water potential gradient can be defined without the mechanical energy term ($\Delta\mu_w^*$), as shown in Fig. 11, across the air/goldenberry surface interface. Furthermore, the chemical potential gradient of the water over the surface of the goldenberry shows an increase until it reaches a maximum value of 7500 J/mol during the first 450 min, after which it begins to decrease until the end of the drying process.

Using Equation (9), it is possible to determine the phenomenological coefficient using the definition of potential in Equation (10). The accuracy of the phenomenological coefficient increases when the influence of mechanical energy variations at the interface is negligible compared to the energy changes driven by water activity and temperature. According to Traffano-Schiffo et al. (2014), the relationship between the phenomenological coefficient and the water flow will be more linear the smaller the effect of the pressure term (mechanical). Fig. 12 shows this relationship and indicates that it is possible to establish a linear relationship between the two.

With the linear relationship between the coefficient and the flow, the chemical potential can be recalculated from the equation obtained. By subtracting this chemical potential of water from that calculated in Equation (9), as shown in Equation (10), it is possible to determine the mechanical term.

$$v_w\Delta P = \Delta\mu_w - \Delta\mu_w^* \tag{10}$$

Fig. 13 shows the evolution of the mechanical term over the drying time. In the first 100 min, the mechanical term decreases from 1556.259 ± 273.661 to −210.977 ± 175.256, which is related to a large storage of mechanical energy due to the initial contraction of the goldenberry structure caused by the high water loss. From 100 to 600 min, a phase of zero mechanical term is observed, associated with the cellular plasmolysis process. Subsequently, the mechanical energy reaches a value of 2280.527 ± 223.763 at the end of the drying process, releasing mechanical energy to the system.

4. Conclusions

A drying monitoring system using infrared thermography has been developed to follow the drying process of goldenberry to optimum conditions. To this end, the evolution of the emissivity of the fruit surface during the process was obtained.

The evolution of the phenomenological coefficient of goldenberry drying during the process has been obtained, which will allow this operation to be predicted in the future.

The mechanical effect (internal fractures, plasmolysis and storage of mechanical energy) in the goldenberry dehydration process has been observed. This will allow both the rehydration capacity of the fruit and its effect on a formulated food system to be predicted.

Engineering tools such as the sorption isotherm, emissivity and phenomenological coefficient were obtained, which will facilitate future modelling of goldenberry drying.

The integration of infrared thermography with thermodynamic modeling provides a powerful tool for improving the efficiency and control of convective drying processes in the food industry. By enabling non-invasive, real-time monitoring of surface temperature and emissivity, this system allows for better identification of critical drying stages and optimization of process parameters. Furthermore, the quantification

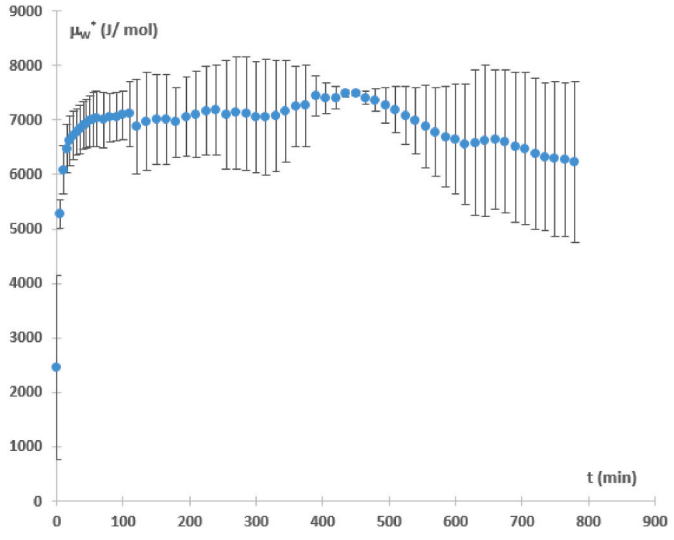

Fig. 11. Evolution of the water chemical potential gradient, without mechanical energy term, between the air and the *Physalis peruviana* surface.

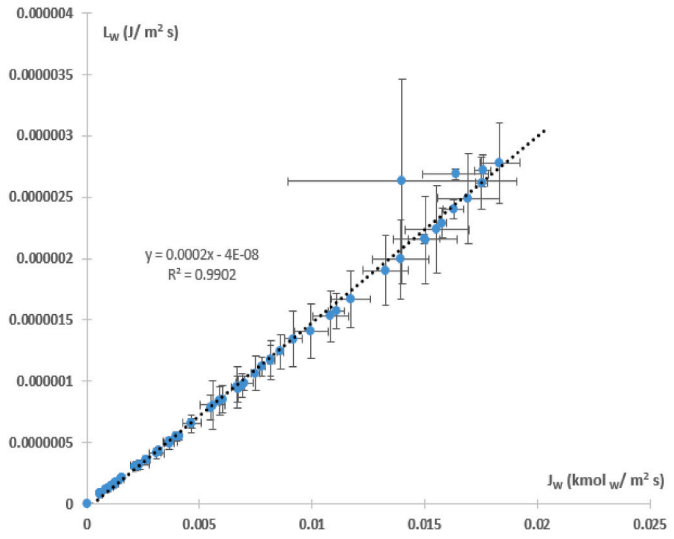

Fig. 12. Relationship between phenomenological coefficient and water flow.

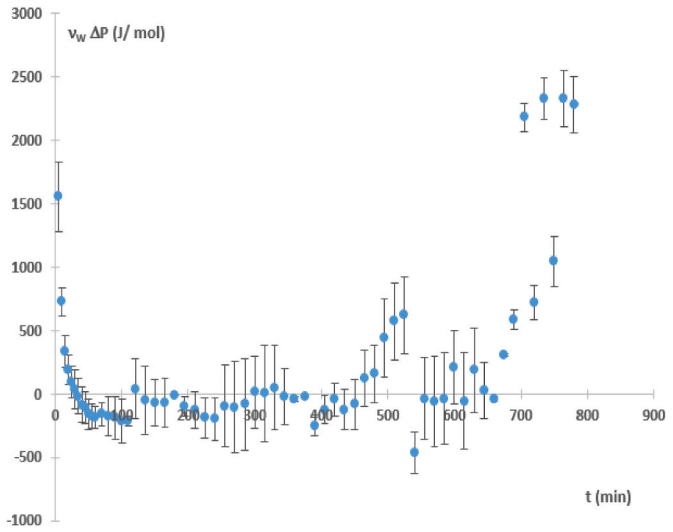

Fig. 13. Evolution of the mechanical energy term of the chemical potential of the water during the whole drying process.

of water flux and chemical potential gradients supports a more accurate prediction of moisture migration, which is crucial for minimizing energy consumption, reducing drying time, and preserving product quality. These findings offer a valuable basis for the development of more sustainable and cost-effective drying protocols for high-moisture fruits such as goldenberry.

CRediT authorship contribution statement

T. Chuquizuta: Writing – original draft, Methodology, Investigation, Formal analysis, Data curation, Conceptualization. **W. Castro:** Writing – review & editing, Validation, Supervision, Methodology, Formal analysis, Data curation, Conceptualization. **M. Castro-Giraldez:** Writing – review & editing, Validation, Supervision, Methodology, Funding acquisition, Formal analysis, Data curation, Conceptualization. **P.J. Fito:** Writing – review & editing, Validation, Supervision, Methodology, Funding acquisition, Formal analysis, Data curation, Conceptualization.

Declaration of competing interest

The authors declare the following financial interests/personal relationships which may be considered as potential competing interests: Pedro J Fito reports financial support was provided by Universitat Politecnica de Valencia. Pedro J Fito reports a relationship with Polytechnic University of Valencia that includes: board membership. If there are other authors, they declare that they have no known competing financial interests or personal relationships that could have appeared to influence the work reported in this paper.

Acknowledgment

Funding for open access charge: Universitat Politècnica de València.

Data availability

Data will be made available on request.

References

Aviara N, A., 2020. Moisture sorption isotherms and isotherm model performance evaluation for food and agricultural products. In Sorption in 2020s. IntechOpen. https://doi.org/10.5772/intechopen.87996.

Akpinar, E.K., Midilli, A., Bicer, Y., 2006. The first and second law analyses of thermodynamic of pumpkin drying process. J. Food Eng. 72 (4), 320–331. https://doi.org/10.1016/j.jfoodeng.2004.12.011.

Avendaño, W.A., Muñoz, H.F., Leal, L.J., Deaquiz, Y.A., Castellanos, D.A., 2022. Physicochemical characterization of cape gooseberry (*Physalis peruviana* L.) fruits ecotype Colombia during preharvest development and growth. J. Food Sci. 87 (10), 4429–4439. https://doi.org/10.1111/1750-3841.16318.

Balaguer, H.E., Fischer, G., Magnitskiy, S., 2024. Chapter 11 - physiology and biochemistry of the Physalis peruviana fruit. In: Fawzy Ramadan, Mohamed (Ed.), Handbook of Goldenberry (Physalis Peruviana). Academic Press, pp. 121–137. https://doi.org/10.1016/B978-0-443-15433-1.00011-X.

Barbosa-Cánovas, G.V., Vega-Mercado, H., 1996. Dehydration of Foods. Springer US. https://doi.org/10.1007/978-1-4757-2456-1.

Bazalar Pereda, M.S., Nazareno, M.A., Viturro, C.I., 2019. Nutritional and antioxidant properties of physalis peruviana L. Fruits from the argentinean northern andean region. Plant Foods Hum. Nutr. 74 (1), 68–75. https://doi.org/10.1007/s11130-018-0702-1.

Blas Saavedra, R., Cruz-Tirado, J.P., Figueroa-Avalos, H.M., Barbin, D.F., Amigo, J.M., Siche, R., 2024. Prediction of physicochemical properties of cape gooseberry (Physalis peruviana L.) using near infrared hyperspectral imaging (NIR-HSI). J. Food Eng. 371, 111991. https://doi.org/10.1016/j.jfoodeng.2024.111991.

Cabrera Ordoñez, Y.A., Estrada Mesa, E.M., Cortés Rodríguez, M., 2017. The influence of drying on the physiological quality of cape gooseberry (Physalis peruviana L.) fruits added with active components. Acta Agronómica 66 (4), 512–518. https://doi.org/10.15446/acag.v66n4.59507.

Cuibus, L., Castro-Giráldez, M., Fito, P.J., Fabbri, A., 2014. Application of infrared thermography and dielectric spectroscopy for controlling freezing process of raw potato. Innov. Food Sci. Emerg. Technol. 24, 80–87. https://doi.org/10.1016/j.ifset.2013.11.007.

Doymaz, İ., 2008. Convective drying kinetics of strawberry. Chem. Eng. Process. Process Intensif. 47 (5), 914–919. https://doi.org/10.1016/j.cep.2007.02.003.

ElGamal, R.A., Kishk, S.S., ElMasry, G.M., 2017. Validation of CFD models for the deep-bed drying of rice using thermal imaging. Biosyst. Eng. 161, 135–144. https://doi.org/10.1016/j.biosystemseng.2017.06.018.

Fischer, G., Herrera, A., Almanza, P.J., 2011. Cape gooseberry (Physalis peruviana L.). In: Postharvest Biology and Technology of Tropical and Subtropical Fruits. Elsevier, pp. 374–397e. https://doi.org/10.1533/9780857092762.374.

Fischer, G., Martinez, O., 1999. Calidad y madurez de la uchuva (Physalis peruviana l.) en relación con la coloración del fruto. Agron. Colomb. 16 (1–3), 35–39.

Fletcher, N.H., 1970. The Chemical Physics of Ice. Cambridge University Press. https://doi.org/10.1017/CBO9780511735639.

Garavito, J., Herrera, A.O., Castellanos, D.A., 2021. A combined mathematical model to represent transpiration, respiration, and water activity changes in fresh cape gooseberry (Physalis peruviana) fruits. Biosyst. Eng. 208, 152–163. https://doi.org/10.1016/j.biosystemseng.2021.05.015.

Gowen, A.A., Tiwari, B.K., Cullen, P.J., McDonnell, K., O'Donnell, C.P., 2010. Applications of thermal imaging in food quality and safety assessment. Trends Food Sci. Technol. 21 (4), 190–200. https://doi.org/10.1016/j.tifs.2009.12.002.

Hidayat, D.D., Luthfiyanti, R., Iwansyah, A.C., Herminiati, A., Rahman, T., Rahman, N., Andriansyah, R.C.E., 2021. Identification and evaluation of physical and mechanical properties of Physalis peruviana L. IOP Conf. Ser. Earth Environ. Sci. 672 (1), 012056. https://doi.org/10.1088/1755-1315/672/1/012056.

İzli, N., Yıldız, G., Ünal, H., Işık, E., Uylaşer, V., 2014. Effect of different drying methods on drying characteristics, colour, total phenolic content and antioxidant capacity of <scp>G</scp> oldenberry (<*scp*>*P*<*/scp*> *hysalis peruviana* <scp>L</scp> .). Int. J. Food Sci. Technol. 49 (1), 9–17. https://doi.org/10.1111/ijfs.12266.

Junqueira, J.R. de J., Corrêa, J.L.G., de Oliveira, H.M., Ivo Soares Avelar, R., Salles Pio, L.A., 2017. Convective drying of cape gooseberry fruits: effect of pretreatments on kinetics and quality parameters. LWT - Food Sci. Technol. (Lebensmittel-Wissenschaft -Technol.) 82, 404–410. https://doi.org/10.1016/j.lwt.2017.04.072.

Kraiem, A., Madiouli, J., Shigidi, I., Sghaier, J., 2023. Experimental analysis of drying conditions' effect on the drying kinetics and moisture desorption isotherms at several temperatures on food materials: corn case study. Processes 11 (1), 184. https://doi.org/10.3390/pr11010184.

Kylili, A., Fokaides, P.A., Christou, P., Kalogirou, S.A., 2014. Infrared thermography (IRT) applications for building diagnostics: a review. Appl. Energy 134, 531–549. https://doi.org/10.1016/j.apenergy.2014.08.005.

Lerman, P., Scheepers, G., 2023. Determination of a mass-transfer coefficient for wood drying by means of thermography. Wood Mater. Sci. Eng. 18 (6), 2104–2111. https://doi.org/10.1080/17480272.2023.2243473.

Lombraña, J.I., Rodríguez, R., Ruiz, U., 2010. Microwave-drying of sliced mushroom. Analysis of temperature control and pressure. Innov. Food Sci. Emerg. Technol. 11 (4), 652–660. https://doi.org/10.1016/j.ifset.2010.06.007.

Lopez, H.E.B., Fischer, G., Magnitskiy, S., 2024. Physiology and biochemistry of the Physalis peruviana fruit. In: Handbook of Goldenberry (Physalis Peruviana). Elsevier, pp. 121–137. https://doi.org/10.1016/B978-0-443-15433-1.00011-X.

Lopez, J., Vega-Gálvez, A., Torres, M.J., Lemus-Mondaca, R., Quispe-Fuentes, I., Di Scala, K., 2013. Effect of dehydration temperature on physico-chemical properties and antioxidant capacity of goldenberry (Physalis peruviana L.). Chil. J. Agric. Res. 73 (3), 293–300. https://doi.org/10.4067/S0718-58392013000300013.

Motahayyer, M., Arabhosseini, A., Samimi-Akhijahani, H., 2019. Numerical analysis of thermal performance of a solar dryer and validated with experimental and thermographical data. Sol. Energy 193, 692–705. https://doi.org/10.1016/j.solener.2019.10.001.

Muñoz, P., Parra, F., Simirgiotis, M.J., Sepúlveda Chavera, G.F., Parra, C., 2021. Chemical characterization, nutritional and bioactive properties of physalis peruviana

fruit from high areas of the atacama desert. Foods 10 (11), 2699. https://doi.org/10.3390/foods10112699.
Nawirska-Olszańska, A., Stępień, B., Biesiada, A., Kolniak-Ostek, J., Oziembłowski, M., 2017. Rheological, chemical and physical characteristics of golden berry (physalis peruviana L.) after convective and microwave drying. Foods 6 (8), 60. https://doi.org/10.3390/foods6080060.
Obregón La Rosa, A., Talledo Rodríguez, G., Pinedo Taco, R., 2021. Native fruits of Peru as a potential source of nutrients, bioactive compounds and antioxidant capacity in the nutritional requirements of vulnerable groups. Revista de La Facultad de Agronomía, Universidad Del Zulia 38 (2), 421–440. https://doi.org/10.47280/RevFacAgron(LUZ).v38.n2.11.
Ordóñez-Santos, L.E., Martínez-Girón, J., Arias-Jaramillo, M.E., 2017. Effect of ultrasound treatment on visual color, vitamin C, total phenols, and carotenoids content in Cape gooseberry juice. Food Chem. 233, 96–100. https://doi.org/10.1016/j.foodchem.2017.04.114.
Pappalardo, S., Consoli, S., Longo-Minnolo, G., Vanella, D., Longo, D., Guarrera, S., D'Emilio, A., Ramírez-Cuesta, J.M., 2023. Performance evaluation of a low-cost thermal camera for citrus water status estimation. Agric. Water Manag. 288, 108489. https://doi.org/10.1016/j.agwat.2023.108489.
Pasten, A., Gomez-Perez, L.S., Vega-Galvez, A., Uribe, E., Puente, L., 2024. Drying technologies of Physalis peruviana. In: Handbook of Goldenberry (Physalis Peruviana). Elsevier, pp. 351–372. https://doi.org/10.1016/B978-0-443-15433-1.00034-0.
Puente, L.A., Pinto-Muñoz, C.A., Castro, E.S., Cortés, M., 2011. Physalis peruviana Linnaeus, the multiple properties of a highly functional fruit: a review. Food Res. Int. 44 (7), 1733–1740. https://doi.org/10.1016/j.foodres.2010.09.034.
Puente, L., Vega-Gálvez, A., Ah-Hen, K.S., Rodríguez, A., Pasten, A., Poblete, J., Pardo-Orellana, C., Muñoz, M., 2020. Refractance Window drying of goldenberry (Physalis peruviana L.) pulp: a comparison of quality characteristics with respect to other drying techniques. LWT 131, 109772. https://doi.org/10.1016/j.lwt.2020.109772.
Puente, L., Vega-Gálvez, A., Fuentes, I., Stucken, K., Rodríguez, A., Pastén, A., 2021. Effects of drying methods on the characterization of fatty acids, bioactive compounds and antioxidant capacity in a thin layer of physalis (Physalis peruviana L.) pulp. J. Food Sci. Technol. 58 (4), 1470–1479. https://doi.org/10.1007/s13197-020-04659-0.
Ramirez-Hernandez, A., Galagarza, O.A., Álvarez Rodriguez, M.V., Pachari Vera, E., Valdez Ortiz, M. del C., Deering, A.J., Oliver, H.F., 2020. Food safety in Peru: a review of fresh produce production and challenges in the public health system. Compr. Rev. Food Sci. Food Saf. 19 (6), 3323–3342. https://doi.org/10.1111/1541-4337.12647.
Reyes-Chaparro, J.E., Arballo, J.R., Campañone, L.A., 2024. Experimental study of parchment coffee drying using the combined fluidization and microwave process: analysis of drying curves and thermal imaging. J. Food Eng. 383, 112214. https://doi.org/10.1016/j.jfoodeng.2024.112214.
Rossi, D., Fuentes, R., Pardo, F., Reyes, D., Tirado, R., Urbina, E., Vega, J., 2012. Effect of temperature and synergism of sucrose, saccharin and sugar light in osmotic dehydration aguaymanto (Physalisperuviana). Agroindustrial Science 100–109. https://doi.org/10.17268/agroind.science.2012.01.03.
Ruan, J., Li, M., Liu, Y., Ye, B., Ling, C., 2022. Adsorption isotherm and thermodynamic properties of microwave vacuum dried tilapia fillets. LWT 166, 113766. https://doi.org/10.1016/j.lwt.2022.113766.
Talens, C., Arboleya, J.C., Castro-Giraldez, M., Fito, P.J., 2017. Effect of microwave power coupled with hot air drying on process efficiency and physico-chemical properties of a new dietary fibre ingredient obtained from orange peel. LWT 77, 110–118. https://doi.org/10.1016/j.lwt.2016.11.036.
Talens, C., Castro-Giraldez, M., Fito, P.J., 2016a. A thermodynamic model for hot air microwave drying of orange peel. J. Food Eng. 175, 33–42. https://doi.org/10.1016/j.jfoodeng.2015.12.001.
Talens, C., Castro-Giraldez, M., Fito, P.J., 2016b. Study of the effect of microwave power coupled with hot air drying on orange peel by dielectric spectroscopy. LWT - Food Sci. Technol. (Lebensmittel-Wissenschaft -Technol.) 66, 622–628. https://doi.org/10.1016/j.lwt.2015.11.015.
Tomas-Egea, J.A., Castro-Giraldez, M., Colom, R.J., Fito, P.J., 2022. New technique for determining the critical freezing temperatures of chicken breast based on radiofrequency photospectrometry. J. Food Eng. 333, 111155. https://doi.org/10.1016/j.jfoodeng.2022.111155.
Tomas-Egea, J.A., Traffano-Schiffo, M.V., Castro-Giraldez, M., Fito, P.J., 2021. Hot air and microwave combined drying of potato monitored by infrared thermography. Appl. Sci. 11 (4), 1730. https://doi.org/10.3390/app11041730.
Traffano-Schiffo, M.V., Castro-Giraldez, M., Colom, R.J., Fito, P.J., 2015. Study of the application of dielectric spectroscopy to predict the water activity of meat during drying process. J. Food Eng. 166, 285–290. https://doi.org/10.1016/j.jfoodeng.2015.06.030.
Traffano-Schiffo, M.V., Castro-Giráldez, M., Fito, P.J., Balaguer, N., 2014. Thermodynamic model of meat drying by infrarred thermography. J. Food Eng. 128, 103–110. https://doi.org/10.1016/j.jfoodeng.2013.12.024.
Uribe, E., Gómez-Pérez, L.S., Pasten, A., Pardo, C., Puente, L., Vega-Galvez, A., 2022. Assessment of refractive window drying of physalis (Physalis peruviana L.) puree at different temperatures: drying kinetic prediction and retention of bioactive components. J. Food Meas. Char. 16 (4), 2605–2615. https://doi.org/10.1007/s11694-022-01373-7.
Vásquez-Parra, J.E., Ochoa-Martínez, C.I., Bustos-Parra, M., 2013. Effect of chemical and physical pretreatments on the convective drying of cape gooseberry fruits (Physalis peruviana). J. Food Eng. 119 (3), 648–654. https://doi.org/10.1016/j.jfoodeng.2013.06.037.
Vega-Gálvez, A., López, J., Ah-Hen, K., Torres, M., Lemus-Mondaca, R., 2014a. Thermodynamic properties, sorption isotherms and glass transition temperature of cape gooseberry (physalis peruviana L.). Food Technol. Biotechnol. 52 (1), 83–92.
Vega-Gálvez, A., López, J., Ah-Hen, K., Torres, M., Lemus-Mondaca, R., 2014b. Thermodynamic properties, sorption isotherms and glass transition temperature of cape gooseberry (Physalis peruviana L.). Food Technol. Biotechnol. 52 (1), 83–92.
Vega-Gálvez, A., Puente-Díaz, L., Lemus-Mondaca, R., Miranda, M., Torres, M.J., 2014. Mathematical modeling of thin-layer drying kinetics of cape gooseberry (*Physalis peruviana* L.). J. Food Process. Preserv. 38 (2), 728–736. https://doi.org/10.1111/jfpp.12024.
Vega-Gálvez, A., Zura-Bravo, L., Lemus-Mondaca, R., Martinez-Monzó, J., Quispe-Fuentes, I., Puente, L., Di Scala, K., 2015. Influence of drying temperature on dietary fibre, rehydration properties, texture and microstructure of Cape gooseberry (Physalis peruviana L.). J. Food Sci. Technol. 52 (4), 2304–2311. https://doi.org/10.1007/s13197-013-1235-0.
Yasin, O., Aysun, O., Senem, T. uuml fek ccedil i., 2016. Effect of two dipping pretreatment on drying kinetics of golden berry (Physalis peruviana L.). Afr. J. Agric. Res. 11 (1), 40–47. https://doi.org/10.5897/AJAR2014.8937.
Yilmaz, N., Gill, W., Donaldson, A.B., Lucero, R.E., 2008. Problems encountered in fluctuating flame temperature measurements by thermocouple. Sensors 8 (12), 7882–7893. https://doi.org/10.3390/s8127882.
Yıldız, G., İzli, N., Ünal, H., Uylaşer, V., 2015. Physical and chemical characteristics of goldenberry fruit (Physalis peruviana L.). J. Food Sci. Technol. 52 (4), 2320–2327. https://doi.org/10.1007/s13197-014-1280-3.